Video Article

Implantation of Electrospun Vascular Grafts with Optimized Structure in a Rat Model

Kang Qin[1], Yifan Wu[1], Yiwa Pan[1], Kai Wang[1], Deling Kong[1], Qiang Zhao[1]

[1]State Key Laboratory of Medicinal Chemical Biology, Key Laboratory of Bioactive Materials (Ministry of Education), College of Life Sciences, Nankai University

Correspondence to: Kai Wang at 013053@nankai.edu.cn, Qiang Zhao at qiangzhao@nankai.edu.cn

URL: https://www.jove.com/video/57340
DOI: doi:10.3791/57340

Keywords: Biology, Issue 136, Vascular graft, electrospinning, macroporous structure, long-term performance, tissue regeneration, rat abdominal aorta replacement model

Date Published: 6/27/2018

Citation: Qin, K., Wu, Y., Pan, Y., Wang, K., Kong, D., Zhao, Q. Implantation of Electrospun Vascular Grafts with Optimized Structure in a Rat Model. *J. Vis. Exp.* (136), e57340, doi:10.3791/57340 (2018).

Abstract

Here, we present a protocol to fabricate macroporous PCL vascular graft and describe an evaluation protocol by using a rat model of abdominal aorta replacement. The electrospun vascular grafts often possess relatively small pores, which limit cell infiltration into the grafts and hinder the regeneration and remodeling of the neo-arteries. In this study, PCL vascular grafts with thicker fibers (5 - 6 μm) and larger pores (~30 μm) were fabricated by using a modified processing technique. The long-term performance of the graft was evaluated by implantation in a rat abdominal aorta model. Ultrasound analysis showed that the grafts remained patent without aneurysm or stenosis occurring even after 12 months of implantation. Macroporous structure improved the cell ingrowth and thus promoted tissue regenerated at 3 months. More importantly, there was no sign of adverse remodeling, such as calcification within the graft wall after 12 months. Therefore, electrospun PCL vascular grafts with modified macroporous processing hold potential to be an artery substitute for long-term implantation.

Video Link

The video component of this article can be found at https://www.jove.com/video/57340/

Introduction

Vascular grafts made from synthetic polymers are widely utilized in clinic for the therapy of cardiovascular diseases (CVDs). Unfortunately, in the case of small-diameter vascular grafts (*D* <6 mm) there are no successful products available due to the low patency triggered by reduced blood flow velocity, which often leads to thrombosis, intimal hyperplasia, and other complications[1].

Tissue engineering provides an alternative strategy to realize long-term patency and homeostasis based on a scaffold-guided vascular regeneration and reconstruction. In detail, the vascular graft, as a three-dimensional template, could provide mechanical support and structural guidance during the regeneration of vascular tissue and influence cellular functions, including cell adhesion, migration, proliferation, and secretion of extracellular-matrix[2]. Up to now, various synthetic polymers have been evaluated for applications in vascular tissue engineering. Among these polymers, poly(ε-caprolactone) (PCL) has been intensively investigated due to good cell compatibility and slow degradation ranging from several months to two years[3]. In a rat aorta model[4,5,6], PCL vascular grafts processed by electrospinning exhibited excellent structural integrity and patency, as well as continuously increased cell invasion and neovascularization in the graft wall for up to 6 months. However, adverse tissue remodeling, including regression of cells and capillaries and calcification, were also observed at longer timepoints, up to 18 months.

Cellularization of the vascular graft is a key factor determining tissue regeneration and remolding[7]. Electrospinning, as a versatile technique, has been widely employed for the preparation of vascular grafts with nano-fibrous structure[8]. Unfortunately, the relatively small pore structure often leads to insufficient cell infiltration in the electrospun vascular graft, which limits the subsequent tissue regeneration. To resolve this problem, various techniques have been attempted to increase pore size and overall porosity, including the salt/polymer leaching[9,10], modification of collector apparatus, post-treatment by laser radiation[11], *etc*. In fact, the structure of electrospun grafts (including fiber diameter, pore size, and porosity) is closely related to the processing conditions[12,13]. During electrospinning, the fiber diameter can be readily controlled by changing the parameters, such as the concentration of the polymer solution, flow rate, voltage, *etc*.[14,15], and therefore, the pore size and porosity have been enhanced accordingly.

We recently reported a modified PCL electrospun graft with macroporous structure (fibers with diameter of 5 - 7 μm and pores of 30 - 40 μm). *In vivo* implantation by replacing rat abdominal aorta showed high rate of patency, as well as good endothelialization and smooth muscle regeneration at 3 months post-surgery[16]. More importantly, no adverse tissue remodeling including calcification and cell regression could be observed even after one year of implantation.

Protocol

The use of experimental animals was approved by the Animal Experiments Ethical Committee of Nankai University and carried out in conformity with the Guide for Care and Use of Laboratory Animals.

1. Fabrication of Electrospun PCL Grafts

NOTE: Herein, an electrospinning technique was utilized to fabricate vascular grafts.

1. Prepare PCL solutions of 25 wt% and 10 wt%, by dissolving PCL in a mixture of methanol and chloroform, respectively, (1:5 volume ratio), at room temperature (RT) for 12 h.
2. Load the PCL solution into a 10-mL glass syringe.
3. Place the syringe with a 21-G needle.
4. Place the stainless-steel mandrel (2 mm in diameter, 25 cm in length) on the collection instrument.
5. For thicker-fiber grafts, use the PCL solution of 25 wt%, working distance of 17 cm from needle tip to collector, flow rate of 8 mL/h, and voltage of 11 kV as the electrospinning parameters. For thinner-fiber grafts, use the PCL solution of 10 wt%, working distance of 20 cm from needle tip to collector, a flow rate of 2 mL/h, and voltage of 18 kV as the electrospinning parameters.
6. Ensure that the obtained grafts are placed in vacuum overnight to remove the residual solvent. Sterilize all instruments prior to the procedure and maintain aseptic technique throughout.
7. Prior to the implantation, disinfect the grafts by immersing them in 10 mL of 75% ethanol for 30 min and then exposing them to UV light overnight.
8. Fiber and pore size measurements: Calculate the average fiber diameter using ImageJ software based on scanning electron microscopy (SEM) images.
9. Mechanical testing of scaffolds:
    1. Cut the tubular scaffolds into 3 mm sections in length using a razor blade. Measure the thickness of scaffolds using a micrometer.
    2. Place the tubular scaffolds on a tensile-testing machine with a load capacity of 100 N.
    3. Clamp the scaffolds with a 1 mm inter-clamp distance and pull longitudinally at a rate of 10 mm/min until rupture. Measure the tensile strength and ultimate elongation at break. Calculate Young's modulus from the initial linear region (up to 5% strain) of the stress-strain curve.

2. Rat Abdominal Aorta Implantation Model

NOTE: All materials and instruments used in surgery are sterile. During the surgery, make sure that the operator wears a gauze mask and sterile gloves to avoid infections. Ensure the room temperature is kept at 27 - 30 °C to maintain the animal body temperature. Follow local IACUC guidelines regarding analgesia.

1. Use male Sprague Dawley rats weighing 240 - 270 g as recipients of vascular graft. Ensure the rat has fasted 24 h before surgery. The aim of fasting rats for 24 h is to empty the faeces in the intestinal tract sufficiently, thereby broaden the operator’s horizon.
2. Grasp the rat's back neck and keep its head downwards, insert the springe needle into the abdominal cavity of the lower abdomen. Induce the rat for anesthesia with chloral hydrate (330 mg/kg) by an intraperitoneal injection.
3. Confirm adequate anesthetization by ensuring that the rat has relaxed muscles and steady breathing. Place the rat under the operating microscope in a supine position.
4. Apply petrolatum ophthalmic vet ointment on the eyes to prevent dryness while under anesthesia. Administer anticoagulation (100 UI/kg) with heparinized physiological saline solution (50 UI/mL) by tail vein injection before surgery.
5. Shave off the fur in the anterior abdominal wall using a razor blade, and clean the skin using Iodine solution and medical alcohol solution.
6. Perform a midline laparotomy incision with surgical scissors and ensure that the incision is about 4 - 5 cm long, and then expose the abdominal cavity.
7. Retract and wrap the intestines with gauze moistened with saline solution preferentially.
8. Dissect the abdominal aorta carefully.
9. Identify and ligate all small branches using 9-0 monofilament nylon sutures.
10. Clamp the isolated section (up to 1 cm in length) of the aorta using two vascular clamps. The aorta can remain clamped for 20-30 min.
11. Transect the abdominal aorta between two clamps using micro-scissors to create the anastomotic sites.
12. Flush the two ends of aorta using heparinized saline (50 UI/mL) solution to remove the residual blood.
13. Peel off the adventitia using micro-scissors.
14. Anastomose the graft with 2 mm inner diameter and 1 cm in length to the rat's abdominal aorta with a figure-of-eight suture pattern using 9-0 monofilament nylon sutures.
15. Firstly, construct four anastomoses according to the sequence of 9, 3, 12, and 6 o'clock positions at the proximal side, then anastomose the cut edges in 4 stitches between two sutures. After finishing the proximal suture, suture the distal side by the same method.
    NOTE: Every stitch is required to ensure the native side is slightly embedded in the graft.
16. Remove the distal clamp to allow the blood to flow into the graft, then remove the proximal clamp.
17. Press the suture ends to stop the bleeding using a sterile cotton ball or a small gauze sponge. Press for about 3 min, until hemostasis.
18. Return the intestines into the abdominal cavity.
19. Flush the abdominal cavity using warm physiological saline solution with gentamicin (320 U/mL).
20. Sew up the abdominal wall using a 3-0 Nylon suture in the muscle and skin layer, respectively.
21. Place the rat into a clean and dry cage and put a heating pad under the cage to maintain animal body temperature; then wait for the rat to recover from anesthesia. Attend to the animal until it has regained sufficient consciousness to maintain sternal recumbency.

22. After it regains consciousness, put the rat in a single cage with food and water. Apply iodine on the wound to prevent infection after surgery. Return the rat to the company of other animals until it fully recovers.
23. Euthanize rats according to institutional guidelines at predetermined time points.

Representative Results

The PCL grafts were explanted at 3 months and 12 months post-operatively and analyzed by standard histological techniques for hematoxylin and eosin (H&E), Masson trichrome, Verhoeff-van Gieson (VVG), Von Kossa, and immunofluorescence staining for α-SMA, MYH, vWF, and elastin. The histological images were taken using an upright microscope, and the immunofluorescence images were taken using a fluorescence microscope.

All data were expressed as mean ± SD. A two-tailed paired Student's *t*-test was used to compare the differences. A value of $p < 0.05$ was considered to be statistically significant.

Novel electrospun PCL grafts with optimized structure, that is, thicker fibers and larger pores, were successfully fabricated in this study. SEM images demonstrated that the averaged fiber diameter was almost 8 times thicker in the modified grafts (**Figure 1A**) than in the conventional one (**Figure 1B**) (5.59 ± 0.67 versus 0.69 ± 0.54 μm). As a result, the averaged pore size was markedly increased, from ~ 4.66 μm in thinner-fiber graft to ~ 40.88 μm in the thicker-fiber one. Cross-sections showed homogeneous fiber distribution within the wall of the tubular grafts in both thicker-fiber (**Figure 1D-F**) and thinner-fiber groups (**Figure 1G-I**). The wall thickness was about 400 - 500 μm. The mechanical properties of grafts were characterized by tensile testing, and the typical stress-strain curves were shown in **Figure 1C**. The mechanical properties of two grafts were evidently different in terms of elongation. The corresponding value of thicker-fiber grafts was about 3 times higher than the thinner-fiber grafts, suggesting the enhanced toughness.

The prepared vascular grafts (inner diameter of 2.0 mm and length of 1 cm) (**Figure 2A**) were implanted to replace a segment of native abdominal aorta in rat (**Figure 2B**). At predetermined time points, the patency of the implanted grafts was examined by ultrasound. Results showed that most of the grafts were patent (**Figure 2C**). Further, the velocity of blood flow was similar between the graft and adjacent native blood vessels at 12 months. Explanted grafts retained good morphology without aneurysm (**Figure 2D**), and no stenosis or thrombi could be observed on the luminal surface (**Figure 2E**).

Tissue regeneration and ECM secretion at 3 months were further assessed by histology analyses. H&E staining showed that a layer of neo-tissue was formed on the lumen of the graft (**Figure 3G-H**). Furthermore, vWF staining show that the luminal surface was fully covered by newly formed endothelium (**Figure 3A**), resembling that of the native aorta (**Figure 3B**). Meanwhile several layers of MYH-positive cells were organized along the circumferential direction, indicating the regeneration of vascular media (**Figure 3C-D**). Extracellular matrix synthesis was observed by Masson and VVG staining, respectively. A significant amount of collagen and fibrous elastin could be observed within the graft (**Figure 3I-J**, **K-L**), which plays an important role in vascular regeneration and remodeling. Immunofluorescence staining further showed the structure of elastin was aligned circumferentially in a pattern like that in the native artery (**Figure 3E-F**).

Furthermore, the regenerated tissues including endothelium and smooth muscle maintained integrated and did not regress after 12 months of implantation (**Figure 4A-C**). More importantly, there was no sign of calcification occurring within the graft wall based on the Von Kossa staining (**Figure 4D**).

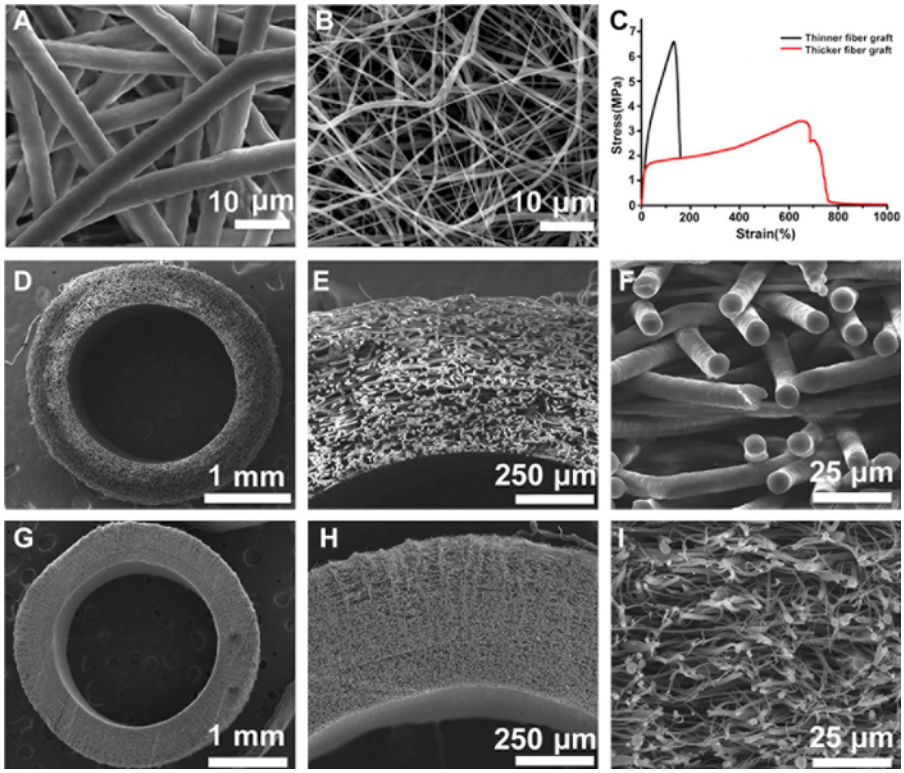

Figure 1: The structure and mechanical property of the PCL graft. SEM images of electrospun PCL mats with thicker fibers (**A**) and thinner fibers (**B**). Cross-sections of thicker-fiber tubular grafts (**D-F**) and thinner-fiber grafts (**G-I**). The representative strain-stress curve is shown in (**C**). These figures have been modified from Zhao, *et al.*[16] Please click here to view a larger version of this figure.

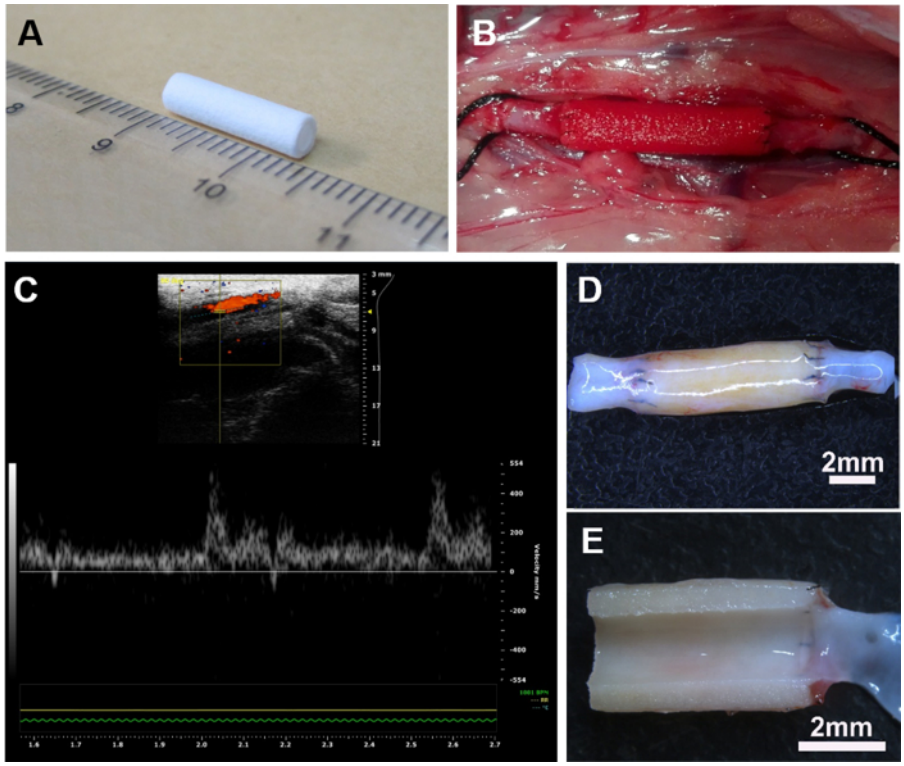

Figure 2: Implantation of vascular grafts in a rat abdominal aorta model. Electrospun PCL vascular graft of 1 cm in length (**A**) was surgically interposed into the abdominal aorta in rat (**B**). The ultrasound image showed that the graft was patent *in vivo* at 1 year (**C**). Stereomicroscopic images show that the graft was well-integrated with adjacent native aorta without aneurysm (**D**), and the luminal surface is clean and free of thrombus (**E**). Please click here to view a larger version of this figure.

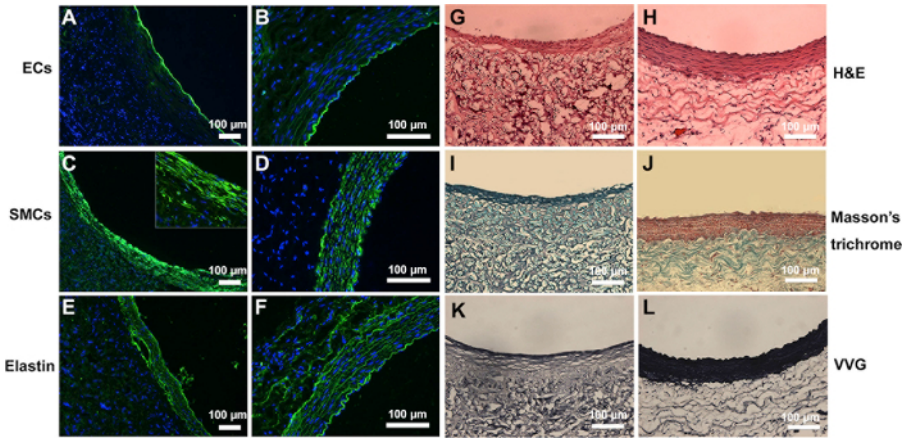

Figure 3: Tissue regeneration and deposition of ECM in the explanted grafts at 3 months in comparison with native aorta. Cross-sectional images of the regenerated grafts (**A**, **C**, and **E**) and native artery (**B**, **D**, and **F**) were immunostained to detect the endothelial cells, smooth muscle cells, and elastin. H&E staining shows the tissue regeneration in the explanted grafts (**G**) compared to native aorta (**H**). Masson's staining revealed that the presence of collagen in the explanted grafts (**I**) and native aorta (**J**). VVG staining showed the presence of elastin in the explanted grafts (**K**) and native aorta (**L**). These figures have been modified from Zhao, *et al.*[16] Please click here to view a larger version of this figure.

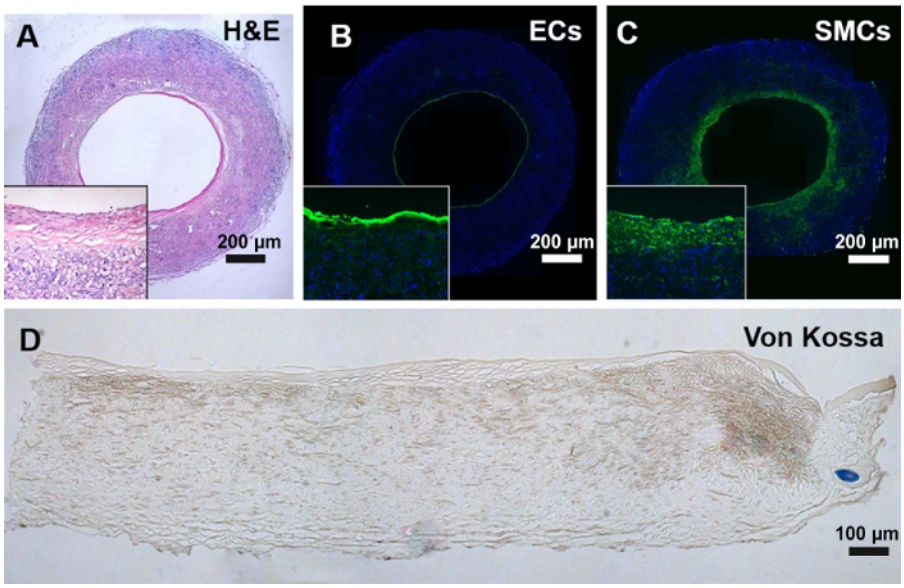

Figure 4: Histological analysis of the explanted grafts at 12 months. (**A**) H&E staining showed the tissue regeneration in the explanted grafts. (B) Endothelium was immunostained by vWF antibody. (**C**) Smooth muscle was immunostained by α-SMA antibody. (**D**) Calcification was evaluated by Von Kossa staining. Please click here to view a larger version of this figure.

Discussion

Cell infiltration is critical for the regeneration and remodeling of the vascular graft *in vivo*[16]. Limited cell infiltration is often related to the relatively small pores of the graft that hinder the migration of cells into the graft wall. To address this difficulty, we developed a modified method to prepare electrospun PCL vascular grafts with large-pore structure. In detail, the pore size increased with the increase of fiber thickness that could be readily controlled by the processing parameters. The results showed that the host cells could easily infiltrate into the wall of this macroporous graft after *in vivo* implantation and the cellularity remained at a relatively high level without obvious cell regression at 12 months post-surgery.

Native artery mainly consists of three layers, that is, endothelium, tunica media, and adventitia. Endothelium, as an anti-thrombogenic interface, plays a vital role in maintaining the long-term patency of the blood vessel. In our study, full endothelialization on the graft was observed at 3 months. In addition, the tunica media consisting of several layers of smooth muscle cells are very important in regulating blood vessel function and providing appropriate mechanical properties of the artery. The present study revealed that the electrospun PCL grafts with thick-fiber and large pore markedly enhanced the regeneration of functional tunica media. Besides, the structure of regenerated smooth muscle is similar to that of the native tunica media. Immunofluorescence staining showed several layers of MYH^+ cells distributed within elastin network, reflecting the contractile phenotype of smooth muscle cells circumferentially. More importantly, regenerated tissues (both endothelium and smooth muscle) kept intact and there was no adverse remodeling even after 12 months due to the imbalance between ECM synthesis and degradation.

Calcification is still a major problem associated with cardiovascular implants, especially in the vascular graft. Vascular smooth muscle cells (VSMCs) lose their original phenotype and experience trans-differentiation towards osteochondrogenic direction, leading to ectopic mineralization during the process of vascular calcification. Our study showed that there was no calcium deposition occurring within the graft wall even after 12 months of implantation. The main reasons for the inhibited calcification in the macro-porous vascular graft include: (1) the structure of the macro-porous graft promotes metabolism, such as ion exchange between cells and blood; (2) the physical cues of the graft structure could regulate or inhibit the differentiation of the VSMC into the osteoblast[1], (3) good cell infiltration in the large pores promotes the secretion of the ECM and inhibits its degradation that will trigger calcification[17], and (4) normal or functional VSMCs have a potential to prevent the calcium deposition[18].

In summary, the long-term evaluation of macro-porous electrospun PCL vascular grafts in the rat abdominal aorta model provides important insight into potential challenges of degradable vascular grafts, which will direct the following research.

Disclosures

The authors have no conflicting financial interests.

Acknowledgements

This work was financially supported by NSFC projects (81522023, 81530059, 91639113, 81772000, 81371699, and 81401534).

References

1. Coombs, K. E., Leonard, A. T., Rush, M. N., Santistevan, D. A., & Hedberg-Dirk, E. L. Isolated effect of material stiffness on valvular interstitial cell differentiation. *J Biomed Mater Res A.* **105** (1), 51-61 (2017).
2. Zhang, L. *et al.* A sandwich tubular scaffold derived from chitosan for blood vessel tissue engineering. *J Biomed Mater Res A.* **77** (2), 277-284 (2006).
3. Thottappillil, N., & Nair, P. D. Scaffolds in vascular regeneration: current status. *Vasc Health Risk Manag.* **11** 79-91 (2015).
4. Pektok, E. *et al.* Degradation and healing characteristics of small-diameter poly (e-caprolactone) vascular grafts in the rat systemic arterial circulation. *Circulation.* **118** (24), 2563-2570 (2008).
5. Innocente, F. *et al.* Paclitaxel-eluting biodegradable synthetic vascular prostheses: a step towards reduction of neointima formation? *Circulation.* **120** (11 Suppl), S37-45 (2009).
6. de Valence, S. *et al.* Advantages of bilayered vascular grafts for surgical applicability and tissue regeneration. *Acta Biomater.* **8** (11), 3914-3920 (2012).
7. Assmann, A. *et al.* Acceleration of autologous in vivo recellularization of decellularized aortic conduits by fibronectin surface coating. *Biomaterials.* **34** (25), 6015-6026 (2013).
8. Hasan, A. *et al.* Electrospun scaffolds for tissue engineering of vascular grafts. *Acta Biomater.* **10** (1), 11-25 (2014).
9. Baker, B. M. *et al.* The potential to improve cell infiltration in composite fiber-aligned electrospun scaffolds by the selective removal of sacrificial fibers. *Biomaterials.* **29** (15), 2348-2358 (2008).
10. Wang, K. *et al.* Creation of macropores in electrospun silk fibroin scaffolds using sacrificial PEO-microparticles to enhance cellular infiltration. *Journal of Biomedical Materials Research Part A.* **101** (12), 3474-3481 (2013).
11. Lee, B. L. P. *et al.* Femtosecond laser ablation enhances cell infiltration into three-dimensional electrospun scaffolds. *Acta Biomaterialia.* **8** (7), 2648-2658 (2012).
12. Rnjak-Kovacina, J., & Weiss, A. S. Increasing the pore size of electrospun scaffolds. *Tissue Eng Part B Rev.* **17** (5), 365-372 (2011).
13. Zhong, S., Zhang, Y., & Lim, C. T. Fabrication of large pores in electrospun nanofibrous scaffolds for cellular infiltration: a review. *Tissue Eng Part B Rev.* **18** (2), 77-87 (2012).
14. Pham, Q. P., Sharma, U., & Mikos, A. G. Electrospun poly(epsilon-caprolactone) microfiber and multilayer nanofiber/microfiber scaffolds: characterization of scaffolds and measurement of cellular infiltration. *Biomacromolecules.* **7** (10), 2796-2805 (2006).
15. Rnjak-Kovacina, J. *et al.* Tailoring the porosity and pore size of electrospun synthetic human elastin scaffolds for dermal tissue engineering. *Biomaterials.* **32** (28), 6729-6736 (2011).
16. Wang, Z. *et al.* The effect of thick fibers and large pores of electrospun poly(epsilon-caprolactone) vascular grafts on macrophage polarization and arterial regeneration. *Biomaterials.* **35** (22), 5700-5710 (2014).
17. Hutcheson, J. D. *et al.* Genesis and growth of extracellular-vesicle-derived microcalcification in atherosclerotic plaques. *Nat Mater.* **15** (3), 335-343 (2016).
18. Tara, S. *et al.* Well-organized neointima of large-pore poly(L-lactic acid) vascular graft coated with poly(L-lactic-co-epsilon-caprolactone) prevents calcific deposition compared to small-pore electrospun poly(L-lactic acid) graft in a mouse aortic implantation model. *Atherosclerosis.* **237** (2), 684-691 (2014).

